Friction and Wear Properties of Amorphous Carbon Nitride Coatings in Water Lubrication

Zhou Fei(周飞)[1,2,3*], *Koji Kato*[4]

1. State Key Laboratory of Mechanics and Control of Mechanical Structures, Nanjing University of Aeronautics and Astronautics, Nanjing, 210016, P. R. China;
2. College of Mechanical and Electrical Engineering, Nanjing University of Aeronautics and Astronautics, Nanjing, 210016, P. R. China;
3. Jiangsu Key Laboratory of Precision and Micro-Manufacturing Technology, Nanjing University of Aeronautics and Astronautics, Nanjing, 210016, P. R. China;
4. Laboratory of Tribology, School of Mechanical Engineering, Nihon University, Fukushima, 963-8642, Japan

(Received 12 August 2014; revised 26 September 2014; accepted 30 September 2014)

Abstract: The friction and wear properties of amorphous carbon nitride (a-CN_x) coatings in water lubrication were reviewed. The influences of mating materials and tribological variables such as normal load (W) and sliding speed (V) on the friction and wear properties of the a-CN_x coatings were analyzed. It was indicated that the specific wear rate of the a-CN_x coatings was related to the hydration reaction of mating materials with water. If the mating materials were easily hydrated, the specific wear rate of a-CN_x coatings was low. The water-lubricated properties of the a-CN_x coatings were better in comparison to the a-C coatings. The a-CN_x/Si-based non-oxide ceramics tribo-pairs exhibited the lowest friction coefficient and wear rate. To describe their friction and wear properties at the normal loads of 3—15 N and the sliding speeds of 0.05—0.5 m/s, the wear-mechanism maps for the a-CN_x/SiC (Si_3N_4) tribo-pairs in water were developed.

Key words: amorphous carbon nitride (a-CN_x) coatings; friction; wear; water lubrication

CLC number: TH117 **Document code**: A **Article ID**: 1005-1120(2014)05-0463-15

1 Introduction

Oil-based lubrication systems have been widely used in the modern driving systems. However, the leakage of oil from synthetic devices can pollute the natural environments. To prevent this pollution source, nature has produced water-based lubrication systems through the process of natural selection. However, water-based lubrication systems actually have some technical problems, including controllability, tribology, corrosion and reliability. Since a very low friction coefficient ($\leqslant$0.002) was found in water lubricated friction Si_3N_4 sliding against itself with pin-on-disk apparatus[1], Si-based non-oxidation ceramic water lubrication has already displayed the high potential for industrial applications such as journal bearings and mechanical face seals for water pumps. If the ceramic water-lubrication tribo-pairs could be used to replace the metal oil-lubrication system in modern machine designs, the problems of environmental pollution and resource shortages will be greatly improved. As is known, the friction coefficient lower than 0.01 was obtained for self-mated Si-based non-oxidation ceramics and the wear mechanism changed from mechanically dominated wear to tribochemical wear thanks to smoothening the surface[2-3].

Foundation items: Supported by the National Natural Science Foundation of China (50675102, 50975137, 51375231); the Program for New Century Excellent Talents in University (NCET-10-068); the Research Fund for the Doctoral Program of Higher Education (20133218110030); the Priority Academic Program Development of Jiangsu Higher Education Institutions (PAPD); Japan Society for the Promotion of Science under Grant-in-Aid for Scientific Research (JSPS Fellows P03219).

* **Corresponding author**: Zhou Fei, Professor, E-mail: fzhou@nuaa.edu.cn.

However, due to the longer running-in period for SiC/SiC tribo-pairs in water and the easy occurrence of hydration reaction between SiC (Si_3N_4) and water, severe wear was easily observed for the self-mated SiC (Si_3N_4) tribopair in water[4-5]. Moreover, the high cost and difficult fabrication of engineering ceramics usually restrict their applications in industries. An alternative approach is to take advantage of metallic materials that is relatively inexpensive and easy to machine. The required tribological properties of metal in water could be improved via depositing hard coatings with good lubricity in water environment.

Since Liu, et al. in 1989 predicted theoretically that the carbon nitride compound (β-C_3N_4) might be harder than diamond[6], many attempts to obtain the carbon nitride films have already been performed[7-12]. Nevertheless, until now, nearly all CN_x films grown at room temperature are amorphous mixtures of carbon and carbon nitride phases with x ranging from 0.1 to 0.5[13-14]. Nitrogen incorporation in the carbon coatings decreases the fraction of sp^3 carbon bonds by the formation of C—N, C=N and C≡N bonds. Previously, the micro- and macro-tribological properties of the a-CN_x coatings have been investigated when the a-CN_x coatings slid against SiC, Si_3N_4, Al_2O_3 and steel in various gases[15-31]. Recently, the water-lubricated properties of the a-CN_x coatings have been concerned[32-40]. It is most imperative to know the influence of mating balls and tribological variables on the friction and wear properties of the amorphous carbon nitride (a-CN_x) coatings in water.

In this viewpoint, this paper introduces our recent experimental results and overviews the potential of CN_x coatings for tribological usage in water.

2 Coating Procedure and Structure of CN_x Coatings

The a-CN_x and a-C coatings were deposited on Si(100) wafers and SiC (Si_3N_4) disks using ion beam assisted deposition (IBAD). The deposition rate was 2 nm/s, which was controlled via adjusting the emission current of carbon vapor. The acceleration voltage of nitrogen ions was in the range from 1.0 kV to 1.5 kV and the current density of the nitrogen ion beam from 90 to 100 $\mu A/cm^2$. The background pressure was lower than 2.0×10^{-4} Pa and the operating pressure during coating was 7.0×10^{-3} Pa. Carbon vapor was formed via heating a graphite target with an electron beam evaporator. The coating thickness was 0.5 μm. The surface roughness Ra of coatings on the Si-based ceramics measured with surface profilometer varied from 9 to 25 nm. As seen in Fig. 1, the CN_x coatings of 400 nm has an amorphous structure and the interlayer between coating and Si-wafer has a thickness of 5—10 nm.

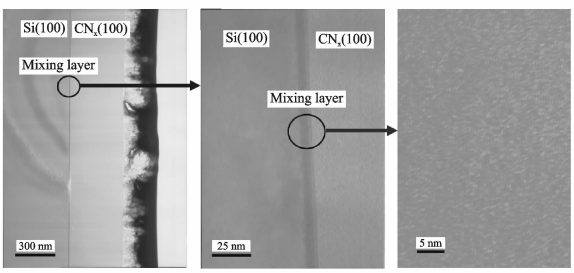

Fig. 1 Cross-sectional FE-TEM image of CN_x coatings on Si wafer

The auger electron spectra (AES) analysis of two coatings was illustrated in Fig. 2. It was clear that the Auger electron energy of carbon hybrided with nitrogen in the a-CN_x coating reduced. The a-CN_x coatings contained 12 at.% nitrogen. As seen in Fig. 3, each Raman spectrum had a broad and skew peak ranging from 1 200 cm^{-1} to 1 700 cm^{-1}, which was composed of the overlapped D-peak (centered round 1 300—1 450 cm^{-1}) and the G-peak (centered round 1 550—1 580 cm^{-1}). The curves-fitted Raman data (Table 1) displayed that the G-peak shifted to higher frequencies while the D-peak shifted to lower frequencies after nitrogen ion bombardment. Furthermore, the intensity ra-

Table 1 D- and G-peak frequencies and their intensity ratio[37]

Coating	ω_D/cm^{-1}	ω_G/cm^{-1}	I_D/I_G
a-C	1 375	1 560	1.07
a-CN_x	1 350	1 575	1.11

tio between D-band and G-band (I_D/I_G) increased from 1.07 to 1.11. This indicated that the sp^2 fraction increased after the nitrogen atoms were incorporated into the a-C coatings[41].

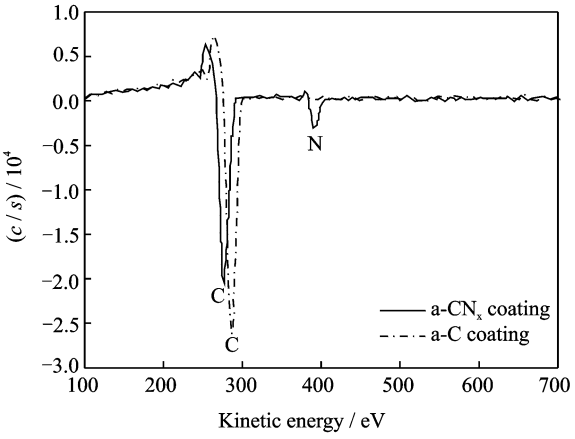

Fig. 2 AES of a-C and a-CN_x coatings[37]

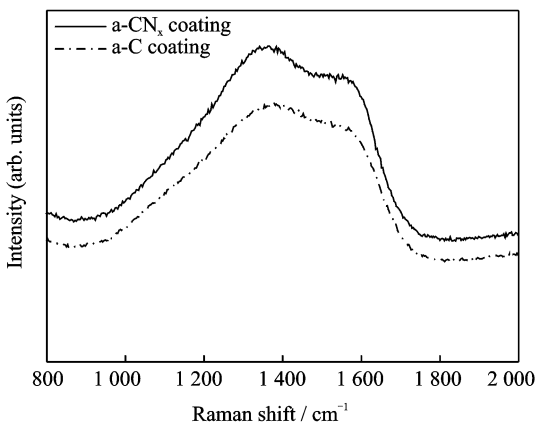

Fig. 3 Raman spectra of a-C and a-CN_x coatings[37]

In order to know the chemical bonding configurations of nitrogen doped into the carbon network, the individual C1s and N1s lines were deconvoluted into Gaussian line shapes (Fig. 4). As seen in Fig. 4, the C1s line was deconvoluted into three peaks at binding energies of 285.1, 286.5 and 288 eV, and the N1s line was deconvoluted into four peaks at binding energies of 398.5, 400.3, 401.5 and 404 eV. Scharf, et al.[22] reported that, for the a-$CN_{0.14}$ coatings, the peaks at binding energies of 284.5, 285.2, 286.5 and 288.6 eV for the deconvoluted C1s spectra were attributed to C=C, C=N, C—N, and C—O bonds, respectively, while the peaks at 398.6, 400.1 and 402.3 eV for the N1s line were assigned to C—N, C=N and N—O bonds, respectively. In comparison to the above-mentioned bonds[22], the peaks at 285.1, 286.5 and 288 eV in Fig. 4(a) were assigned to C=N/C=C, C—N, and C—O bonds, respectively, while the peaks at 398.5, 400.3, 401.5 and 404 eV in Fig. 4(b) were marked as C—N, C=N and N—O bonds, respectively. The appearance of C—O and N—O bonds displayed the coatings' surface contaminated by oxygen from air. It was concluded that the sp^3 C—N and sp^2 C=N/C=C bonds were the major component in the a-CN_x coatings.

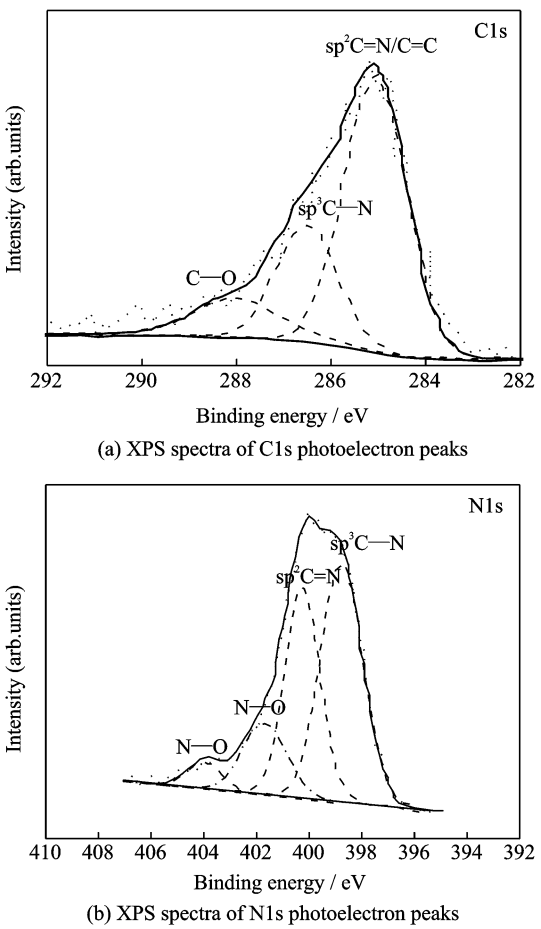

Fig. 4 XPS spectra of C1s photoelectron peaks and N1s photoelectron peaks for a-CN_x coatings[40]

In Table 2, the arithmetic mean roughness Ra and the maximum roughness Ra_{max} of the a-CN_x coatings was a little lower than those of the a-C coatings. This indicated that the energetic particle bombardment enhanced the mobility of carbon atoms on the growing surface and induced the smooth surface. Fig. 5 displayed the nano-

indentation load vs. indentation displacement curves for two carbon coatings. The maximum indentation depth of the a-C coatings was less than that of the a-CN_x coatings at the same load. Based on the standard Oliver and Pharr approach[42], the elastic modulus (E) and hardness (H) for the a-C and the a-CN_x coatings were calculated from Fig. 5 and listed in Table 2. This pointed out that the hardness and Young's modulus of the a-C coatings were higher than those of the a-CN_x coatings, while the ratio of hardness and elastic modulus (H/E) for the a-C coatings was less than that of the a-CN_x coatings. This implied that the a-C coatings were hard and stiff, while the a-CN_x coatings offered a combination of reasonably high hardness and reduced stiffness with a remarkable elastic recovery. Leyland, et al[43]. reported that a high ratio of H/E was indicative of good wear resistance in a disparate range of materials. It is clear from Tables 1, 2 that the nitrogen incorporation in carbon increased the sp^2 carbon bonds' fraction so that the tribological property of the films was improved (low friction coefficient and better durability).

Table 2 Surface roughness and mechanical properties of a-C and a-CN_x coatings[37]

Name	Ra /μm	R_{max}/μm	H/GPa	E/GPa	H/E
a-C	0.011	0.025	34±3	440±15	0.08
a-CN_x	0.009	0.018	29±2	330±20	0.09

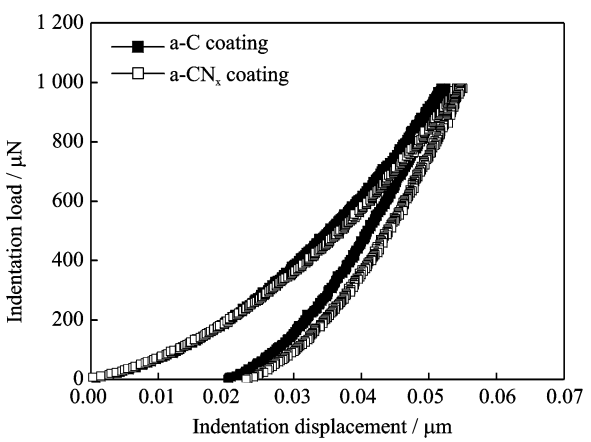

Fig. 5 Nano-indentation load vs. indentation displacement curves for a-C and a-CN_x coatings[37]

3 Influence of Mating Balls on Tribological Properties of a-CN_x Coatings in Water

Fig. 6(a) displays the friction behaviors of the a-CN_x coatings sliding against five kinds of mating balls in water. When the sliding cycles increased, the friction coefficient for the Al_2O_3/a-CN_x tribo-couples first increased to a maximum value of 0.11, and then decreased to 0.10. Finally it varied in the range of 0.087 to 0.11. For the Si-based ceramics/a-CN_x tribopair, the friction coefficients decreased abruptly with an increase in sliding cycles. The friction coefficients of the Si_3N_4/a-CN_x tribo-couples reached a stable value of 0.011 after the amount of sliding cycles was beyond 20 000, while those for the SiC/a-CN_x tribo-pairs reached a minimum value of 0.01 at 10 000 cycles, and then varied in the range of 0.013 to 0.02. When the sliding cycles exceeded 65 000 cycles, the friction coefficients of the Si_3N_4/a-CN_x tribopairs were lower than those of the SiC/a-CN_x tribopairs. For the steel balls/a-CN_x tribopairs, the obvious difference was that the running-in period of the SUS440C/a-CN_x tribo-couples was 500 cycles, while that of the SUJ2 ball/a-CN_x tribo-systems was 55 000 cycles. After running-in, the stable friction coefficient of the SUJ2/a-CN_x tribo-pair was around 0.072, slightly less than that of the SUS440C/a-CN_x tribopairs (0.075). The mean steady-state friction coefficients for five kinds of tribopairs are shown in Fig. 6(b). As the a-CN_x coatings slid against ceramic balls, the Al_2O_3/a-CN_x tribopairs had the highest mean stable friction coefficient of 0.10, while the a-CN_x/SiC(Si_3N_4) tribo-couples had the lowest mean stable friction coefficient. For the steel balls/a-CN_x tribopairs, the mean friction coefficient of the SUS440C/a-CN_x tribopairs was 0.075, slightly higher than that of the SUJ2/a-CN_x tribo-pair (0.072).

The specific wear rates of the a-CN_x coatings after sliding against ceramic balls and steel balls in water are illustrated in Fig. 7(a). Among three kinds of ceramic ball's tribo-pairs, the specific

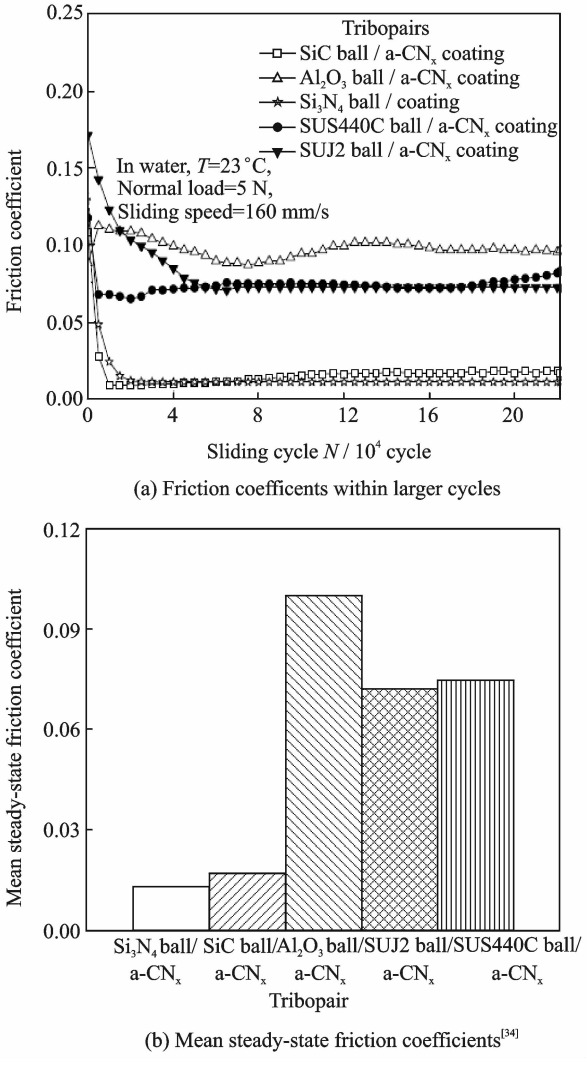

Fig. 6 Friction behaviors of a-CN_x coatings sliding against different mating balls at 5 N and 160 mm/s in water

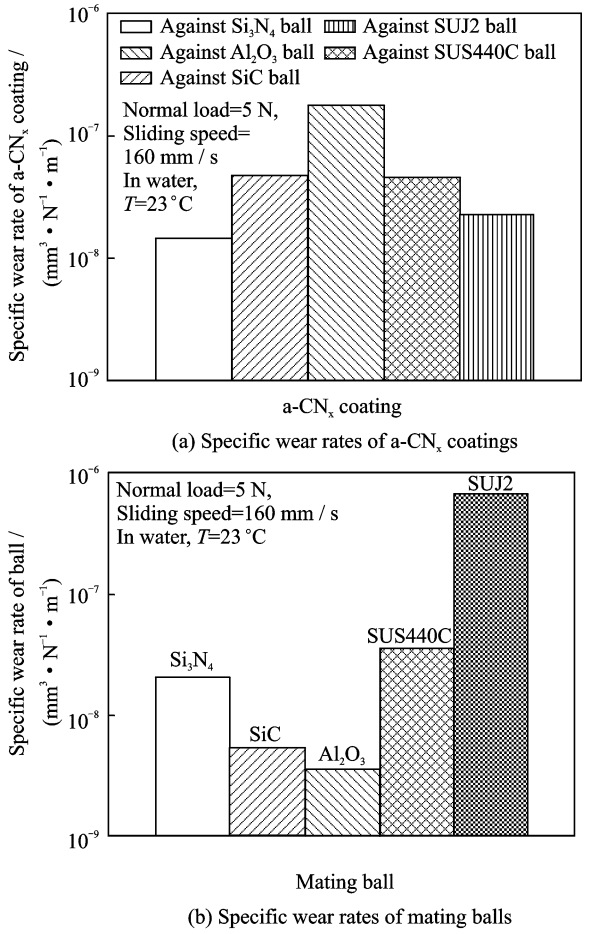

Fig. 7 Specific wear rates of a-CN_x coatings and mating balls[34]

wear rate of the a-CN_x coatings was the highest as sliding against Al_2O_3 ball. However, when silicon nitride was mating ball, the specific wear rate of the a-CN_x coatings was the lowest. For the tribo-systems with steel balls, the specific wear rate of the a-CN_x coatings sliding against SUS440C ball was twice higher than that against SUJ2 ball. Fig. 7(b) illustrates the specific wear rates of mating balls. For ceramic balls, Al_2O_3 ball had the lowest wear rate, while Si_3N_4 ball had the highest one. The specific wear rate of SiC ball was slightly higher than that of Al_2O_3 ball, but four times lower than that of Si_3N_4 ball. For steel balls, the specific wear rate of SUJ2 ball was 20 times higher than that of SUS440C. When Al_2O_3, SiC and SUS440C balls were used as mating materials, the specific wear rate of the a-CN_x coatings was higher than that of their mating ball. On the contrary, as Si_3N_4 and SUJ2 balls were used as mating materials, the specific wear rate of the a-CN_x coatings was less than that of their mating ball, which indicated that the wear rate of the a-CN_x coatings was mainly governed by the chemical properties of mating balls. When the ball materials had an excellent anti-oxidation ability, the main wear occurred in the a-CN_x coatings. For easily oxidative materials such as SUJ2, the main oxidative wear occurred in SUJ2 ball.

To know which tribopair possesses the excellent tribological properties, Figs. 6(b), 7 were rearranged as Fig. 8. It is clear that the tribopairs of the a-CN_x/SiC(Si_3N_4) tribopairs have the low friction coefficient and low wear rate. In the

viewpoint of tribology, the a-CN_x/SiC (Si_3N_4) tribopairs are useful in water.

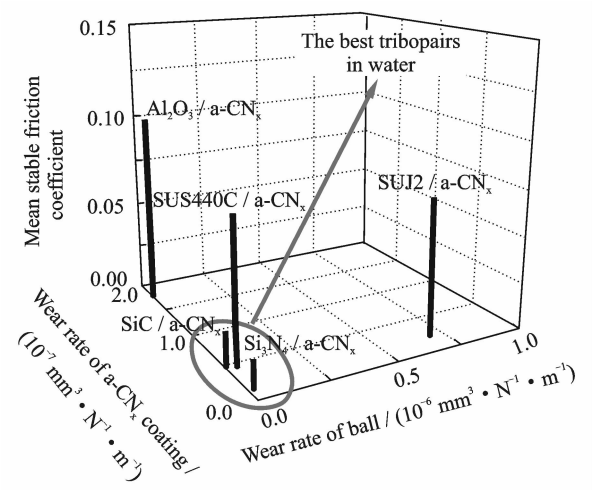

Fig. 8 Influence of mating balls on the tribological properties of a-CN_x coatings in water

4 Comparison of Tribology of a-CN_x/SiC and SiC/SiC Tribopairs in Water

Fig. 9(a) shows the friction coefficient variation for two kinds of tribopairs with sliding cycles in water at various normal loads. At the normal loads of 3—10 N, the friction coefficient of SiC/SiC tribopairs gradually decreased from higher initial value (0.325) to steady-state values (0.010—0.058). But for the a-CN_x/SiC tribopairs, their friction coefficient decreased rapidly from 0.107 to steady-state values (0.02—0.051). Fig. 9(b) exhibits the influence of normal load on the mean steady-state friction coefficients after running-in in water. When the normal load increased, the mean steady-state friction coefficient of SiC/SiC system first decreased, reaching a minimum value at 7 N, then increased. For the a-CN_x/SiC tribopairs, their mean steady-state friction coefficient decreased a little, and then increased gradually as the normal load exceeded 5 N. When the normal load was lower than 5 N or equal to 10 N, the mean steady-state friction coefficients of the SiC/SiC tribopairs were higher than those of the a-CN_x/SiC tribopair, but became lower at 7 N.

The variation of the specific wear rates for

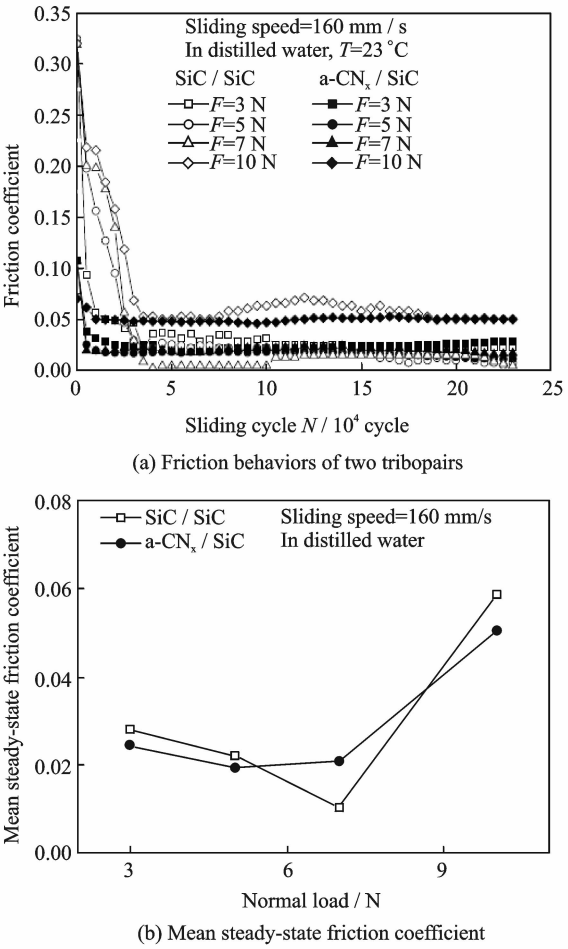

Fig. 9 Friction behaviors of a-CN_x/SiC and SiC/SiC tribopairs at various normal loads[33]

tribomaterials with normal loads are illustrated in Fig. 10. For the a-CN_x/SiC tribopairs, the specific wear rates of SiC ball and the a-CN_x coatings increased linearly with the normal load. However, for the SiC/SiC tribopairs, the transition load (7 N) was observed. When the normal loads were lower than 7 N, the specific wear rates for SiC ball and SiC disk decreased, generally linear with the normal load. If the normal load exceeded 7 N, they obviously increased. It is very interesting that the wear resistance of the SiC ball against the a-CN_x coating was enhanced by a factor up to 100—1 000 in comparison to that against SiC disk in water. The lower wear rate of the SiC ball as sliding against the a-CN_x coatings in water will open up some new interesting field of application. For example, the a-CN_x/SiC tribopairs could be used in seals, sliding bearings for surface protection in water pump or biotechnology.

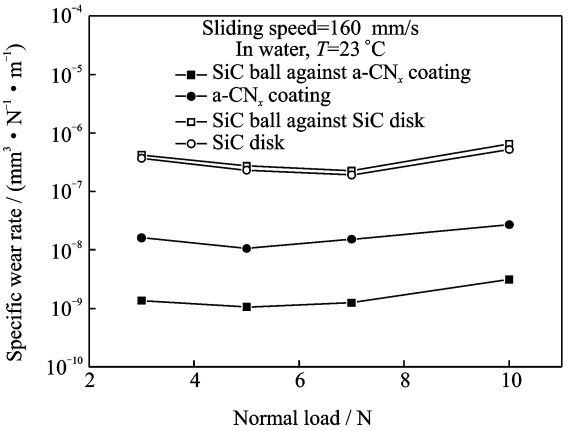

Fig. 10 Variation of specific wear rates with normal loads for a-CN_x/SiC and SiC/SiC tribopairs in water[33]

5 Friction and Wear Properties of a-CN_x/Si_3N_4 Tribopairs in Water

The friction behaviors of the a-CN_x coatings as sliding against Si_3N_4 balls at various normal loads in water are illustrated in Fig. 11(a). In general, the friction coefficient decreased during the early stage of the test and then approached a steady-state value. At a lower normal load of 1.5 N, the initial friction coefficient of the a-CN_x/Si_3N_4 tribopair was 0.25, but when the normal load was higher than 2.5 N, the initial friction coefficient of the a-CN_x/Si_3N_4 tribopair varied in the range from 0.10 to 0.13. As seen in Fig. 11(a), the running-in period of the a-CN_x/Si_3N_4 tribopair varied with the normal load at a sliding velocity of 0.16 m/s. The running-in period was 12 500 cycles at 1.5 N, 13 000 cycles at 2.5 N, 9 020 cycles at 3.5 N and 12 500 cycles at 5 N, respectively. After running-in, the friction coefficient fluctuated in the range of 0.002 to 0.02. Fig. 3(b) shows the influence of normal load on the mean steady-state friction coefficients after running-in for the a-CN_x/Si_3N_4 tribopairs in water. It is clear that the mean steady-state friction coefficient varied around 0.02 or so when the normal load was lower than 3.5 N. At the highest normal load of 5 N, the mean steady-state friction coefficient decreased abruptly from 0.018 to 0.007. The above friction behaviors indicate

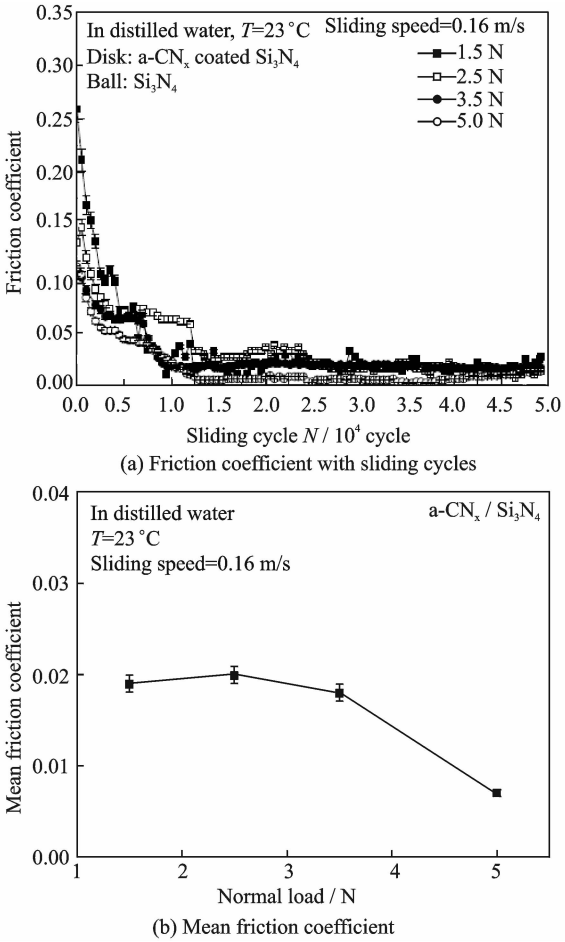

Fig. 11 Friction behaviors of a-CN_x/Si_3N_4 tribopairs at various normal loads[38]

that the a-CN_x/Si_3N_4 tribopairs have excellent frictional characteristics in water lubrication.

In order to know the influence of the a-CN_x coatings on the specific wear rates of Si_3N_4 ceramics in water, the wear behavior of the a-CN_x/Si_3N_4 tribopairs was compared with that of self-mated Si_3N_4 ceramics. The experimental results are illustrated in Fig. 12. It was clear that the specific wear rates of all tribo-materials decreased gradually when the normal load increased from 1.5 N to 5 N. For the a-CN_x/Si_3N_4 tribopair, the specific wear rate of the a-CN_x coatings varied in the range of 3.89×10^{-8} mm³/(N • m) to 7.89×10^{-8} mm³/(N • m), a little higher than that of the Si_3N_4 balls. Moreover, the specific wear rates of the a-CN_x coatings and the Si_3N_4 balls all were at the lowest level of 10^{-8} mm³/(N • m). But for the self-mated Si_3N_4 tribopairs, the specific wear rates of the Si_3N_4 balls fluctuated in the range of

1.28×10^{-6} mm^3/(N·m) to 2.79×10^{-6} mm^3/(N·m), and was approximately twice as high as that of the Si_3N_4 disk, whose specific wear rate varied in the range of 6.18×10^{-7} mm^3/(N·m) to 9.64×10^{-7} mm^3/(N·m). Furthermore, the specific wear rates of the Si_3N_4 balls as sliding against the a-CN_x coating reduced by a factor up to 35 compared to those against Si_3N_4 in water. This indicates that the a-CN_x coatings can enhance the wear resistance of silicon nitride ceramics in water.

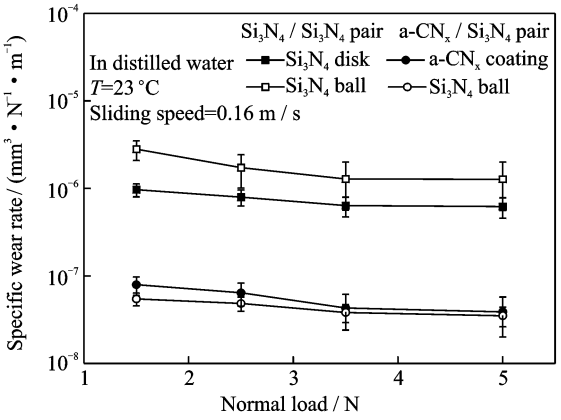

Fig. 12 Variation of specific wear rate with normal loads for a-CN_x/ Si_3N_4 tribopairs in water[38]

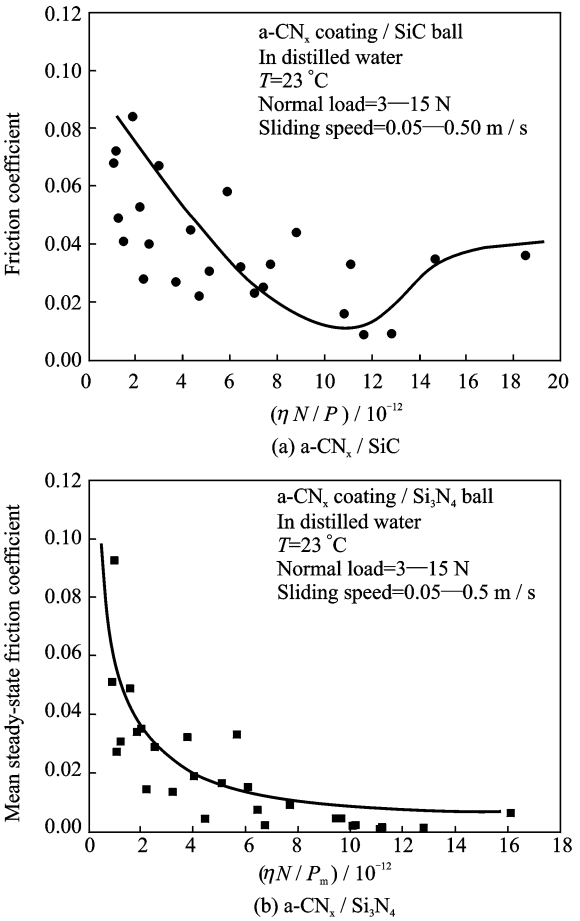

Fig. 13 Stribeck curves of a-CN_x/SiC[35] and a-CN_x/Si_3N_4[39] tribopair in water after running-in

6 Water-Lubricated Mechanism and Wear Mechanism Map of a-CN_x/SiC(Si_3N_4) Tribo pairs

Fig. 13 shows the relationship between friction coefficient and Sommerfeld number $\eta N/P$ (P is mean contact pressure, N is rotating velocity, η is viscosity of lubricant)[35,39]. It is clear that there existed a critical sommerfeld number for the a-CN_x/SiC tribo-couple. With an increase in Sommerfeld number, the friction coefficient for the a-CN_x/SiC tribo-couple decreased gradually to 0.012 or so, and then increased to a constant value. This pointed out that the water-lubricated mechanism changed from boundary lubrication (BL) to mix lubrication (ML), then changed from ML to hydrodynamic lubrication (HL). However, for the a-CN_x/Si_3N_4 tribopairs, when a Sommerfeld number was lower than the critical value, the friction coefficient increased abruptly to 0.093 when the Sommerfeld number decreased. When the Sommerfeld number was higher than the critical value, the friction coefficient decreased gradually with an increase in Sommerfeld number, which indicated that the lubrication mechanism changed from ML to BL as the Sommerfeld number decreased. In fact, the dependence relationship between friction coefficient and Sommerfeld number was related to the lubrication film between tribopairs after running-in in water. At higher normal load of 15 N and lower sliding speed of 0.05 m/s, the water lubrication film broke down and the solid-to-solid contact existed, so the friction coefficient increased abruptly and the lubrication mechanism changed into BL. With an increase in sliding speed or decrease in normal load, the water lubrication film would exist at the contact interface, therefore, the friction coefficient decreased rapidly and the water-lubricated mechanism would change from BL to ML or HL.

Fig. 14 shows the wear-mechanism map of the a-CN_x coatings sliding against SiC and Si_3N_4 ball in water, respectively[35,39]. It is clear that the normal load (W) v. s. sliding velocity (V) diagram for the a-CN_x/SiC tribopairs was divided into five regions, while that for the a-CN_x/Si_3N_4 tribopairs was divided into four regions. When the experimental conditions were located at the first area (I), as shown in Fig. 14, the friction coefficients of the a-CN_x/Si_3N_4 tribopairs fluctuated in the range of 0.05—0.072, while those of the a-CN_x/Si_3N_4 tribo-couple varied in the range of 0.032—0.093. The wear rates of coatings and balls in the a-CN_x/SiC tribopairs varied in the range of 7.4×10^{-8}—11.0×10^{-8} and 5.6×10^{-9}—7.0×10^{-9} $mm^3/(N\cdot m)$, but those in the a-CN_x/Si_3N_4 tribopairs fluctuated in the range of 6.5×10^{-8}—18.9×10^{-8} and 2.2×10^{-8}—9.2×10^{-8} $mm^3/(N\cdot m)$, respectively. In addition, the worn surfaces on balls and coatings were covered with many deeper scratch lines parallel to the sliding direction. Furthermore, the a-CN_x coatings were partially delaminated. This indicated that the wear mechanism at the first region (I) was mechanical wear (MW). As the normal load and the sliding velocity all were lower as located in the second region (II), as seen in Fig. 14(a), the friction coefficient and the wear rates of the a-CN_x coating and SiC balls also exhibited the higher values identical to the experimental data in the first area (I). But for the a-CN_x/Si_3N_4 tribopairs (Fig. 14(b)), when the experimental parameters were located in the second area (II), the friction coefficient of the a-CN_x/Si_3N_4 tribo-couple ranged from 0.014 to 0.049, and the specific wear rates of the a-CN_x coating and Si_3N_4 ball fluctuated in the range of 3.0×10^{-8}—20.4×10^{-8} $mm^3/(N\cdot m)$ and 1.4×10^{-8}—2.8×10^{-8} $mm^3/(N\cdot m)$, respectively. The worn surfaces on the ball and the a-CN_x coatings displayed the smoothness and flatness except for some deeper scratches. This pointed out that the wear mechanism in the second area (II) was MW with partial tribochemical wear (MW+PTW). If the

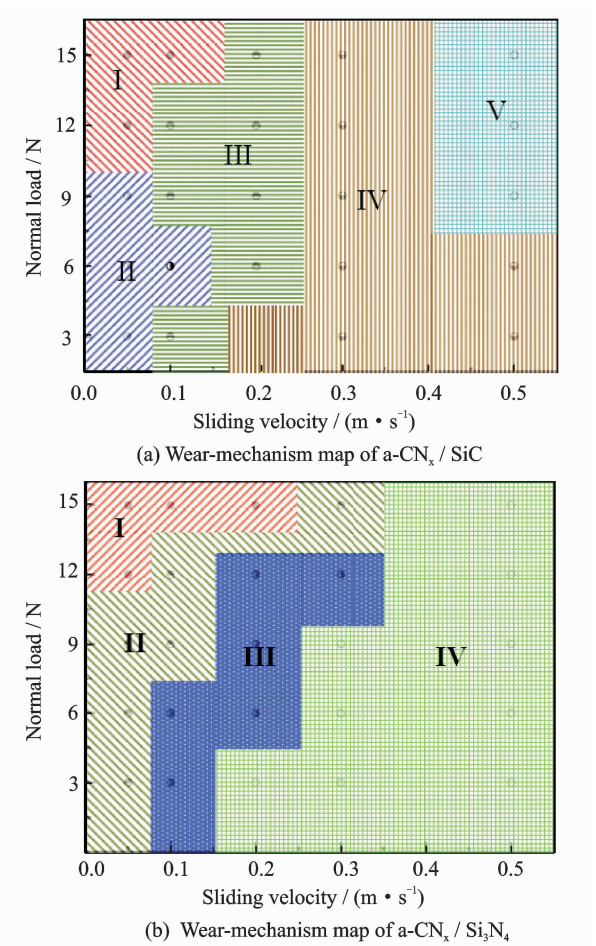

Fig. 14 Wear-mechanism map of a-CN_x coatings sliding against SiC(a)[35] and Si_3N_4(b)[39] balls in water

experimental parameters were located in the third zone (III), the friction coefficient of the a-CN_x/SiC tribopairs varied in the range of 0.03—0.045 and the specific wear rates of the a-CN_x coatings and SiC balls fluctuated in the range of 2.7×10^{-8}—11.0×10^{-8} $mm^3/(N\cdot m)$ and 3.3×10^{-9}—9.5×10^{-9} $mm^3/(N\cdot m)$, and the worn surface became smooth and was covered with some deep scratches. In the third zone, the normal load and the sliding speed just increased slightly, so the extent of tribochemical reaction between tribomaterials and water was not serious. Thus, the wear mechanism was mix wear (partial mechanical wear (PMW) and partial tribochemical wear (PTW))(Fig. 14(a)). However, for the a-CN_x/Si_3N_4 tribopairs, when the experimental parameters were located in the third area (III), the friction coefficient varied in the

range of 0.004—0.029 and the specific wear rate of the a-CN_x coatings and Si_3N_4 balls fluctuated in the range of 3.2×10^{-8}—9.0×10^{-8} $mm^3/(N\cdot m)$ and 1.4×10^{-8}—3.5×10^{-8} $mm^3/(N\cdot m)$. The worn surfaces of Si_3N_4 ball and the a-CN_x coating had become smooth and were covered with shallow scratches. This indicated that a tribochemical reaction had occurred. Thus, the wear mechanism in here was tribochemical wear with slight partial mechanical wear (TW+PMW) (Fig. 14(b)). For the a-CN_x/SiC tribo-couple, as the experimental parameters was in the fourth area (IV), the friction coefficient changed in the range of 0.02—0.04, and the specific wear rates of the a-CN_x coatings and SiC balls fluctuated in the range of 2.0×10^{-8}—5.4×10^{-8} $mm^3/(N\cdot m)$ and 1.5×10^{-9}—3.3×10^{-9} $mm^3/(N\cdot m)$. In this case, the smooth and flat worn surfaces with shallow scratches were observed. This indicated that the wear mechanism was tribochemical wear with a little partial mechanical wear (TW + PMW). If the sliding wear tests were done at the highest normal load and sliding velocity (Zone V), the lowest friction coefficient of 0.009 was obtained at 9—12 N and 0.5 m/s. In the fifth area (V), the friction coefficient was lower than 0.02, and the specific wear rates less than 3.4×10^{-8} $mm^3/(N\cdot m)$ for the a-CN_x coatings and 3.0×10^{-9} $mm^3/(N\cdot m)$ for SiC ball were acquired, and the smooth and flat worn surfaces were observed. Thus, the wear mechanism in the fifth zone was tribochemical wear (TW) (Fig. 14(a)). But for the a-CN_x/Si_3N_4 tribopairs, if the sliding wear tests were performed at the highest sliding velocity (IV), the friction coefficients less than 0.01 as well as the specific wear rates lower than 6.6×10^{-8} $mm^3/(N\cdot m)$ for the a-CN_x coatings and 3.0×10^{-8} $mm^3/(N\cdot m)$ for Si_3N_4 balls were obtained. Besides, smooth and flat worn surfaces were also observed. This made clear that the tribochemical reaction occurred easily, and the $SiO_2\cdot xH_2O$ gels acted as a lubrication film, which was beneficial to providing super lubricity to the self-mated Si_3N_4 tribopairs in water[2]. Thus, the wear mechanism was TW in the fourth zone (Fig. 14(b)).

7 Comparison of Tribological Property of a-C and a-CN_x Coatings Against SiC Balls in Water

Fig. 15(a) shows the variation of friction coefficients for two tribo-pairs in water at 0.16 m/s with various normal loads and sliding cycles. The initial friction coefficient of the a-C/SiC tribopairs was 0.13, higher than that of the a-CN_x/SiC tribopairs (0.11). For the a-C/SiC tribopairs, at a normal load of 3 N, the friction coefficient first decreased suddenly from a higher initial value (0.13) to 0.05, and then fluctuated around 0.06 with a little variation. But after 60 000 cycles, the friction coefficient increased slightly from 0.06 to 0.07. As the normal load became 5 N, the friction coefficient reduced initially from 0.13 to 0.05 within 30 000 cycles, and then varied in the range of 0.05 to 0.06 with further sliding. At a normal load higher than 7 N, the friction coefficient first decreased abruptly from 0.13 to 0.03 at the initial sliding period of 14 000 cycles. With further sliding, the friction coefficient varied around 0.03 or so at 7 N, but it increased gradually from 0.03 to 0.05 at 10 N. For the a-CN_x/SiC tribopairs, the friction coefficient decreased initially from 0.11 to 0.03 within 20 000 cycles, and then varied in the range of 0.02 to 0.03 with further sliding at 3 N. As the normal load was higher than 3 N and lower than 10 N, the friction coefficient decreased markedly from 0.11 to 0.02, and then fluctuated around 0.02 with a little change. If the normal load increased to 10 N, the friction coefficient reduced from 0.11 to 0.05 within 10 000 cycles. After 10 000 cycles, the friction coefficient varied around 0.05 or so with an increase in sliding cycles.

Fig. 15(b) shows the variation of the specific wear rates with the normal load for the SiC balls and the a-C as well as the a-CN_x coatings. In gen-

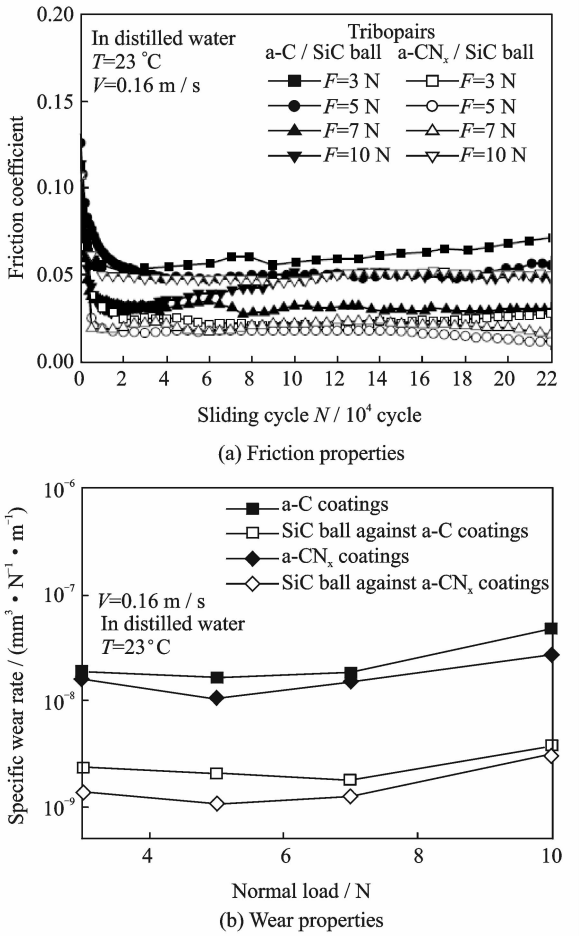

Fig. 15 Friction and wear properties of a-C and a-CN_x coatings against SiC balls in water[37]

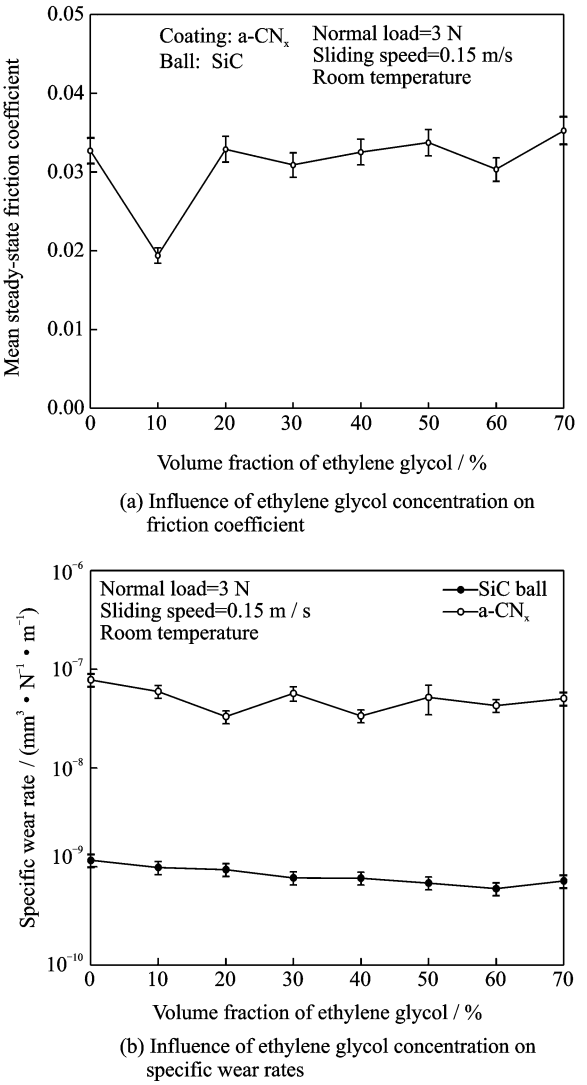

Fig. 16 Influence of ethylene glycol concentration on the friction coefficient and specific wear rates for a-CN_x/SiC tribopairs in aqueous solutions[40]

eral, the specific wear rates of coating and ball in the a-C/SiC tribo-couple were all higher than those of the a-CN_x/SiC tribo-couple, and the wear rates of SiC balls were approximately ten times lower than those of coatings. For the a-CN_x/SiC tribopairs, with an increase in normal load, the specific wear rates first decreased from 1.61×10^{-8} $mm^3/(N\cdot m)$ to 1.05×10^{-8} $mm^3/(N\cdot m)$ for the a-CN_x coatings, and from 1.36×10^{-9} $mm^3/(N\cdot m)$ to 1.05×10^{-9} $mm^3/(N\cdot m)$ for the SiC balls, respectively. As the normal load was higher than 5 N, the specific wear rates all increased obviously from 1.05×10^{-8} $mm^3/(N\cdot m)$ to 2.7×10^{-8} $mm^3/(N\cdot m)$ for the a-CN_x coatings, and from 1.05×10^{-9} $mm^3/(N\cdot m)$ to 3.13×10^{-9} $mm^3/(N\cdot m)$ for the SiC balls. This indicated that the transition load (W_c, above which the specific wear rate increased apparently with a further increase in normal load) of 5 N was observed for the a-CN_x/SiC tribopair. But for the a-C/SiC tribopairs, the specific wear rate of the a-C coatings first decreased slightly from 1.89×10^{-8} $mm^3/(N\cdot m)$ to 1.65×10^{-8} $mm^3/(N\cdot m)$ as the normal load increased from 3 N to 5 N. When the normal load was higher than 5 N, the a-C coatings' wear rates increased markedly from 1.65×10^{-8} $mm^3/(N\cdot m)$ to 4.79×10^{-8} $mm^3/(N\cdot m)$. The SiC ball's wear rate first decreased gradually from 2.36×10^{-9} $mm^3/(N\cdot m)$ to 1.77×10^{-9} $mm^3/(N\cdot m)$ as the normal load increased from 3 N to 7 N, how-

ever, at 10 N, the specific wear rate of SiC ball increased abruptly to 3.68×10^{-9} mm^3/(N·m). In Fig. 15(b), the a-C/SiC tribopair did not show an obvious transition load, but displayed the highest wear rates at 10 N. It is obvious from Fig. 15 that the water-lubricated properties of the a-CN_x coatings were better than the a-C coatings.

8 Influence of Ethylene Glycol Concentration on Tribological Behaviors of a-CN_x/SiC Tribopair

In Fig. 16(a), the mean steady-state coefficient of friction first decreased from 0.033 to 0.019 at 10 vol.%, and then fluctuated slightly in the range of 0.030—0.035 with an increase in the ethylene glycol concentration. Actually, when the ethylene glycol concentration increased, the surface tension of the ethylene glycol solutions decreased, while their viscosity increased. It was concluded that the thickness of lubrication film varied with the ethylene glycol concentration, which induced the variation of coefficient of friction. Fig. 16(b) shows the variation of the specific wear rates of the a-CN_x/SiC tribopair with different ethylene glycol concentrations. When the ethylene glycol concentration increased, the wear rates of SiC ball decreased from 11.2×10^{-10} mm^3/(N·m) to 5.9×10^{-10} mm^3/(N·m), whereas the specific wear rates of the a-CN_x coatings first decreased from 7.8×10^{-8} mm^3/(N·m) to 3.3×10^{-8} mm^3/(N·m) as the ethylene glycol concentration was lower than 20 vol.%, and then fluctuated in the range of 3.3×10^{-8}—5.7×10^{-8} mm^3/(N·m). This indicated that ethylene glycol had more influences on the coefficient of friction and wear rate of the a-CN_x/SiC tribopairs in aqueous solutions.

9 Discussion

As is known, the lower friction coefficients were obtained for SiC/SiC, Si_3N_4/Si_3N_4 and a-CN_x/SiC(Si_3N_4) tribocouples, but the specific wear rates of tribomaterials in the a-CN_x/SiC(Si_3N_4) tribocouples were all lower than those of tribomaterials in the SiC/SiC and Si_3N_4/Si_3N_4 tribocouples. For the a-CN_x/SiC(Si_3N_4) tribo-couples in water, the wear rate of SiC ceramic ball was lower than that of Si_3N_4 ceramic ball[35,39], which indicated that the hydration reaction of Si_3N_4 in water occurred easily. Thermodynamic calculations of the phase equilibrium within the interface showed that water did not react with SiC or Si_3N_4 in the presence of oxygen. Since the water was saturated with oxygen and oxygen was therefore presented in the tribocontact, the following Eqs. (1,2) most likely took place. ΔG_f^{298} is the Gibbs free energy of formation at 298 K

$$SiC+2O_2\rightarrow SiO_2+CO_2$$
$$\Delta G_f^{298}=-589\ \text{kJ/mol} \quad (1)$$
$$Si_3N_4+3O_2\rightarrow 3SiO_2+2N_2$$
$$\Delta G_f^{298}=-1\ 779.4\ \text{kJ/mol} \quad (2)$$

From Eqs. (1,2), it is clear that the formation of SiO_2 film which evolved from Si_3N_4 was expected to be more rapid than SiC tribopairs. The oxides could be hydrated by association with an undetermined amount of water molecules to form $SiO_2\cdot xH_2O$ gels. Such films have been described specifically in the wear experiments of SiC/SiC and Si_3N_4/Si_3N_4 tribo-couples running in moist air[3]. For SiO_2, a subsequent dissolution reaction in the tribo-contact would also be expected to occur

$$SiO_2+2H_2O\rightarrow Si(OH)_4 \quad \Delta G_f^{298}=-237\ \text{kJ/mol} \quad (3)$$

If the hydration reaction between Si_3N_4 or SiC ceramic and water occurred directly, we could calculate from Eqs. (4,5) that silicon nitride was more easily hydrated than silicon carbide

$$SiC+4H_2O\rightarrow Si(OH)_4+CH_4$$
$$\Delta G_f^{298}=-598.91\ \text{kJ/mol} \quad (4)$$
$$Si_3N_4+12H_2O\rightarrow 3Si(OH)_4+4NH_3$$
$$\Delta G_f^{298}=-1\ 268.72\ \text{kJ/mol} \quad (5)$$

This might be attributed to more wear loss on Si_3N_4 than SiC. Ref. [3] proposed that, when a very low friction coefficient was obtained for self-

mated Si_3N_4 tribopairs, there mainly existed $Si(OH)_4$ gels and water film between pin and disk, while for self-mated SiC tribopairs, there existed a SiO_2 film and water film between the two contacting surfaces. Thus, we could conclude that, after the water lubrication film broke down and the $Si(OH)_4$ gels were removed, solid-to-solid contact for the a-CN_x/Si_3N_4 tribopair was established. Hence, the friction coefficient increased abruptly and the lubrication mechanism changed from ML into BL. However, for the a-CN_x/SiC tribocouples, the SiO_2 film acted as a "lubricant" on the worn surface to prevent direct contact of bulk materials, so HL changed into ML and then gradually changed into BL.

Generally, the friction behavior at contact surface was largely governed by the physical condition of the contacting interface and the chemical interactions between the sliding interfaces and the environment. When two dissimilar materials rubbed against each other, the softer materials wore more than the harder, which acquired a layer of transferred softer materials. It is clear that the a-CN_x coatings offered higher values of H/E and a combination of reasonably high hardness and suitable stiffness. Hence they possessed excellent tribological properties. But here, the specific wear rates of the a-CN_x coatings were higher than those of the softer SiC (Si_3N_4) ball in all conditions. This was related to the transfer of a tribo-layer from coating to the ball[44]. Observation of wear scars on the a-CN_x coatings showed that the wear surface became smooth and flat besides some original voids. It indicates that friction transformed the surface layer of coatings and gave it lower shear strength, which was responsible for low friction and the transfer of material. When Tanaka, et al.[45] studied the friction and wear properties of the diamond-like carbon (DLC) coatings in water, they indicated that the structure of transferred materials was very different from that of the original DLC film and similar to that of polymer-like carbon, which is softer in comparison to DLC film. The amount of transferred material with the polymer-like structure was higher in water than in air. However, for the a-CN_x coatings, they were hydrophilic, and the physisorption of water seemed to have a hydrogen-bonded mechanism, by formation of hydrogen bonds between water molecules and nitrogen atoms[46]. It pointed out that nitrogen atoms removed easily from the a-CN_x coating. Ref. [38] has indicated that the nitrogen concentration for the a-CN_x coatings on the worn surface decreased and there were many $sp^2C{=}N$ bonds on the worn surface. Hellgren, et al.[47] have reported that if operated in the presence of oxygen or hydrogen, those elements would react with a-CN_x film and promote decomposition. This indicates that the decomposition of the a-CN_x coatings occurred during sliding in water. After nitrogen atoms removed from the a-CN_x coatings, the sp^2-bonding-rich structure surface with lower shear strength was formed on the worn surface of the a-CN_x films and carbon bonds could be terminated with OH^- in water, which was also responsible for low friction for the a-CN_x/SiC (Si_3N_4) tribocouple, and low wear rate of the SiC (Si_3N_4) ball in water.

10 Conclusions

The fundamental tribological properties of the a-CN_x coatings investigated in the past are reviewed and summarized as follows:

(1) The a-CN_x coatings contained 12 at. % nitrogen and the major chemical bonding of $sp^2C{=}N$ and $sp^3C{-}N$. The nano-hardness of the a-CN_x coatings was 29 GPa.

(2) The a-CN_x/SiC (Si_3N_4) tribopairs possessed the excellent tribological properties in water lubrication, the friction coefficient of the a-CN_x/SiC (Si_3N_4) tribo-pair was lower than 0.05 and the specific wear rates of the a-CN_x coatings and balls all were at a lowest level of 10^{-8} and 10^{-9} $mm^3/(N \cdot m)$.

(3) The wear-mechanism maps for the

a-CN_x/SiC(Si_3N_4) tribopairs in water were developed at the normal loads of 3—15 N and the sliding speeds of 0.05—0.5 m/s.

(4) At a normal load of 3—10 N, the friction coefficients of a-C/SiC tribopair varied in the range of 0.03—0.07, a little higher than those of the a-CN_x/SiC tribopair (0.019—0.05). The specific wear rates of coating and ball in the a-C/SiC ball tribocouple all were higher than those in the a-CN_x/SiC tribopair.

(5) The lowest coefficient of friction of 0.019 was acquired as the ethylene glycol concentration was 10 vol.%.

References:

[1] Tomizawa H, Fischer T E. Friction and wear of silicon nitride and silicon carbide in water: hydrodynamic lubrication at low sliding speed obtained by tribochemical wear[J]. ASLE Trans, 1987(30): 41-46.

[2] Xu J, Kato K. Formation of tribochemical layer of ceramics sliding in water and its role for low friction [J]. Wear, 2000(245): 61-75.

[3] Chen M, Kato K, Adachi K. The comparisons of sliding speed and normal load effect on friction coefficients of self-mated Si_3N_4 and SiC under water lubrication[J]. Tribol Int, 2002(35): 129-139.

[4] Wäsche R, Klaffke D. Ceramic particulate composites in the system SiC-TiC-TiB_2 sliding against SiC and Al_2O_3 under water[J]. Tribol Int, 1999(32): 197-206.

[5] Amutha R D, Yoshizawa Y, Hyuga H, et al. Tribological behavior of ceramic materials (Si_3N_4, SiC and Al_2O_3) in aqueous medium[J]. J Euro Ceram Soc, 2004(24): 3279-3284.

[6] Liu A Y, Cohen M L. Prediction of new low compressibility solids[J]. Science, 1989(245): 841-842.

[7] Kaltofen R, Sebald T, Schulte J, et al. Plasma substrate interaction effects on composition and chemical structure of reactively r. f. magnetron sputtered carbon nitride films[J]. Thin Solid Films, 1999(347): 31-38.

[8] He J L, Chang W L. Carbon nitride films incorporated with metal by rf plasma enhanced chemical vapor deposition[J]. Thin Solid Films, 1998(312): 86-92.

[9] Niu C, Lu Y Z, Lieber C M. Experimental realization of the covalent solid carbon nitride[J]. Science, 1993(261): 334-337.

[10] Krishna M G, Gunasekhar K R, Mohan S J. Low temperature synthesis of thin films of carbon nitride [J]. Mater. Res, 1995(10): 1083-1085.

[11] Aoi Y, Ong K, Kamijo E J. Preparation of amorphous CN_x thin films by pulsed laser deposition using a radio frequency radical beam source[J]. Appl Phys, 1999(86): 2318-2322.

[12] Kohzai M, Matsumuro A, Hayashi T, et al. Preparation of carbon nitride thin films by ion beam assisted deposition and their mechanical properties[J]. Thin Solid Films, 1997(308/309): 239-244.

[13] Zhang Z J, Huang J, Fan S, et al. Phases and physical properties of carbon nitride thin films prepared by pulsed laser deposition[J]. Mater Sci Eng, 1996 (A209): 5-9.

[14] Yoon S F, Rusli J, Ahn J, et al. Deposition of polymeric nitrogenated amorphous carbon films (a-C:H:N) using electron cyclotron resonance CVD[J]. Thin Solid Films, 1999(340): 62-67.

[15] Fernandez-Ramos C, Sayagues M J, RojasT C, et al. Study of the thermal stability of carbon nitride thin films prepared by reactive magnetron sputtering[J]. Diamond & Related Mater, 2000(9): 212-218.

[16] Hellgren H, Lin N, Broitman E, et al. Thermal stability of carbon nitride thin films[J]. J Mater Res, 2001(16): 3188-3201.

[17] Khurshudov A G, Kato K. Tribological properties of carbon nitride overcoat for thin-film magnetic rigid disks[J]. Surf Coating Technol, 1996(86/87): 664-671.

[18] Hajek V, Rusnak K, Vlcek J, et al. Trihological study of CN_x films prepared by reactive d. c. magnetron sputtering[J]. Wear, 1997(213): 80-89.

[19] Wang D F, Kato K. Friction studies of ion beam assisted carbon nitride coating sliding against diamond pin in water vapor[J]. Wear, 1998(217): 307-311.

[20] Czyzniewski A, Precht W, Pancielejko M, et al. Structure, composition and tribological properties of carbon nitride films[J]. Thin Solid Films, 1998 (317): 384-387.

[21] Wei J, Hing P, Mo Z Q. Structure and tribological behavior of carbon nitride films[J]. Wear, 1999 (225/229): 1141-1147.

[22] Scharf T W, Ott R D, Yang D, et al. Structural and tribological characterization of protective amorphous diamond-like carbon and amorphous CN_x overcoats for next generation hard disks[J]. J Appl Phys, 1999 (85): 3142-3154.

[23] Donnet C, Martin J M, Fontaine J, et al. The role of CN chemical bonding on the tribological behavior of

CN_x coatings[J]. Surf Coating Technol, 1999(120/121):594-600.

[24] Kato K, Koide H, Umehara N. Micro-wear properties of carbon nitride coatings[J]. Wear, 2000(328): 40-44.

[25] Bai M, Kato K, Umehara N, et al. Scratch-wear resistance of nanoscale super thin carbon nitride overcoat evaluated by AFM with a diamond tip[J]. Surf Coating Technol, 2000(126):181-194.

[26] Sanchez-Lopez J C, Donnet C, Belin M, et al. Tribochemical effects on CN_x films[J]. Surf Coating Technol, 2000(133/134):430-436.

[27] Hayashi T, Matsumuro A, Muramatsu M, et al. Wear resistance of carbon nitride thin films formed by ion beam assisted deposition [J]. Thin Solid Films, 2000(376):152-158.

[28] BroitmanE, Hellgren N, Wanstrand O, et al. Mechanical and tribological properties of CN_x films deposited by reactive magnetron sputtering[J]. Wear, 2001(248):55-64.

[29] Sanchez-Lopez J C, Donnet C, Le Mogne T. Tribological and surface characterisation in UHV of amorphous CN_x films[J]. Vacuum, 2002(64):191-198.

[30] Sanchez-Lopez J C, Belin M, Donnet C, et al. Friction mechanisms of amorphous carbon nitride films under variable environments: a triboscopic study[J]. Surf Coat Technol, 2002(160):138-144.

[31] Kato K, Umehara N, Adachi K. Friction, wear and N-2-lubrication of carbon nitride coatings: a review [J]. Wear, 2003(254):1062-1069.

[32] Zhou F, Kato K, Adachi K. Effect of a-CN_x coating on tribological properties of SiC ceramic in water[J]. Mater Sci Forum, 2005(475/479):2899-2904.

[33] Zhou F, Kato K, Adachi K. Friction and wear properties of CN_x/SiC in water lubrication [J]. Tribol Lett, 2005(18):153-163.

[34] Zhou F, Adachi K, Kato K. Friction and wear property of a-CN_x coatings sliding against ceramic and steel balls in water[J]. Diamond Relat Mater, 2005 (14):1711-1720.

[35] Zhou F, Adachi K, Kato K. Wear-mechanism map of amorphous carbon nitride coatings sliding against silicon carbide balls in water[J]. Surf Coat Technol, 2006(200):4909-4917.

[36] Zhou F, Adachi K, Kato K. Comparisons of tribological property of a-C, a-CN_x and BCN coatings sliding against SiC balls in water[J]. Surf Coat Technol, 2006(200):4471-4478.

[37] Zhou F, Adachi K, Kato K. Sliding friction and wear property of a-C and a-CN_x coatings against SiC balls in water[J]. Thin Solid Films, 2006(514):231-239.

[38] Zhou F, Wang X, Kato K, et al. Friction and wear property of a-CN_x coatings sliding against Si_3N_4 balls in water[J]. Wear, 2007(263(7-12)):1253-1258.

[39] Zhou F, Wang X, Adachi K, et al. Influence of normal load and sliding speed on the tribological property of amorphous carbon nitride coatings sliding against Si_3N_4 balls in water[J]. Surf Coat Technol, 2008,202(15):3519-3528.

[40] Zhou F, Yue B, Wang Q, et al. Tribological properties of a-CN_x coatings sliding against SiC balls in ethylene glycol aqueous solution [J]. Lubrication Sci, 2010(22):225-236.

[41] Zhang S, Zeng X T, Xie H, et al. A phenomenological approach for the I_D/I_G ratio and sp^3 fraction of magnetron sputtered a-C films[J]. Surf Coat Technol, 2000(123):256-260.

[42] Oliver W C, Pharr G M J. An improved technique for determining hardness and elastic modulus using load and displacement sensing indentation experiment [J]. Mater Res, 1992(7):1564-1583.

[43] Leyland A, Matthews A. Design criteria for wear-resistant nanostructured and glassy-metal [J]. Surf Coat Technol, 2004(177/178):317-324.

[44] Jia K, Li Y Q, Fischer T E, et al. Tribology of diamond-like carbon sliding against itself, silicon nitride, and steel[J]. J Mater Res, 1995(10):1403-1410.

[45] Tanaka A, Suzuki M, Ohana T. Friction and wear of various DLC films in water and air environments[J]. Tribol Lett, 2004(17):917-924.

[46] Zambov L M, Popov C, Plass M F, et al. Capacitance humidity sensor with carbon nitride detecting element[J]. Appl Phys A, 2000(70):603-606.

[47] Hellgren N, Lin N, Broitman E, et al. Thermal stability of carbon nitride thin films[J]. J Mater Res, 2001(11):3188-3201.

(Executive editor: Zhang Tong)